Enhanced spin-density wave in LaFeSbO from first principles

Chang-Youn Moon, Se Young Park, and Hyoung Joon Choi*
Department of Physics and IPAP, Yonsei University, Seoul 120-749, Korea
(Received 14 November 2008; published 24 December 2008)

We predict atomic, electronic, and magnetic structures of a hypothetical compound LaFeSbO by first-principles density-functional calculations. It is shown that LaFeSbO prefers an orthorhombic stripe-type antiferromagnetic phase [i.e., spin-density wave (SDW) phase] to the tetragonal nonmagnetic (NM) phase, with a larger Fe spin moment and greater SDW-NM energy difference than those of LaFeAsO. In the NM-phase LaFeSbO, the electronic bandwidth near the Fermi energy is reduced compared with LaFeAsO, indicating smaller orbital overlap between Fe *d* states and subsequently enhanced intra-atomic exchange coupling. The density of states at the Fermi energy is greatly increased and the calculated Fermi surface in the NM phase shows increased nesting between hole and electron sheets compared with LaFeAsO. Based on monotonous changes found in our calculated material properties of LaFePnO (Pn=P, As, and Sb) along with reported superconducting properties of doped LaFePO and LaFeAsO, doped LaFeSbO is possibly a candidate of superconductor with a higher superconducting transition temperature.

DOI: 10.1103/PhysRevB.78.212507 PACS number(s): 74.70.−b, 71.18.+y, 71.20.−b, 75.25.+z

Since the discovery of an iron-based superconductor LaFePO with a superconducting transition temperature $T_c \sim 4$ K (Ref. 1) and subsequent dramatic increase to 26 K with $LaFeAsO_{1-x}F_x$ compound[2] and to 43 K with external pressure,[3] a huge amount of studies have followed to understand the underlying mechanism of the superconductivity in these iron-based layered oxypnictides and to raise T_c further. This family of materials is characterized by features similar to the cuprate superconductors such as two dimensionality of structural and electronic properties, the antiferromagnetic (AFM) ground state of the undoped parent materials, subsequent loss of the magnetism accompanied by the emergence of the superconductivity with doping, etc. The magnetism is believed to be closely related to the superconductivity in these materials, and a number of theoretical studies have predicted magnetic instability in pure LaFeAsO.[4–8] It is reported that there is a structural phase transition from tetragonal to orthorhombic phase near 150 K and, at temperatures below ~130 K, an AFM order of spin-density wave (SDW) type is identified.[9,10] The existence of SDW state has been confirmed in many other experimental[11–13] and theoretical[11,14–16] works and can be understood by a peculiar Fermi-surface topology, i.e., the Fermi-surface nesting.

Since the conducting FeAs layer is conceived to be the relevant part of magnetism and superconductivity, there have been large efforts to tailor the material by modifying the LaO layer to raise T_c. By substituting La with other rare-earth (RE) elements, series of $REFeAs(O_{1-x}F_x)$ are reported to have T_c of 55 K for RE=Sm,[17] 41 K for RE=Ce,[18] 52 K for RE=Pr,[19] and 50 K for RE=Nd.[20] Besides the fluorine doping, T_c of 53.5 K is reported with GdFeAsO with oxygen deficiency.[21] More recently, $BaFe_2As_2$ and $SrFe_2As_2$, which contain the same FeAs layer as in the REFeAsO compounds but Ba or Sr layer instead of REO layer, have been found to have similar properties of magnetism and superconductivity.[22–25] In these many materials, variations made in the material so far have been restricted to the insulating layer except for FeSe cases, preserving the FeAs layer itself since the first breakthrough of substituting P of LaFePO with As.[2] Considering the great success of As replacing P, an important idea which should be examined is whether or not substituting As with Sb is promising in search for higher T_c; however, there has been no report on this issue.

In this Brief Report, we study the structural, electronic, and magnetic properties of a hypothetical iron-based oxypnictide compound LaFeSbO through first-principles density-functional pseudopotential calculations. We find that the SDW-type AFM spin state is the ground state for this compound similar to existing other oxypnictides LaFePO and LaFeAsO. The crystal structure couples with the magnetic configuration so that the nonmagnetic (NM) phase favors the tetragonal structure; whereas the lower-symmetry orthorhombic structure is favored by the SDW state. The Fermi surface consists of three hole pockets around the Γ point and two electron pockets around the M points, with enhanced nesting between the hole and electron surfaces. We find that LaFeSbO in the SDW phase has a local Fe spin moment larger than that of LaFeAsO, making a trend of monotonous increase from phosphide to antimonide, along with the relative stability of the magnetic ground state with respect to the NM solution. Our calculation suggests LaFeSbO, which is not yet reported to be synthesized, could be a candidate for higher T_c when the spin-fluctuation-mediated superconducting scenario is considered.

Our first-principles calculations are based on the density-functional theory (DFT) within the generalized gradient approximation (GGA) for the exchange-correlation energy functional[26] and the *ab initio* norm-conserving pseudopotentials as implemented in SIESTA code.[27] Semicore pseudopotentials are generated using electronic configurations $5s^2 5p^6 5d^0 6s^0$ with $5s$ and $5p$ electrons as valence electrons and $3s^2 3p^6 3d^6 4s^0$ with $3s$, $3p$, and $3d$ electrons as valence electrons, for La and Fe, respectively. Electronic wave functions are expanded with localized pseudoatomic orbitals (double zeta polarization basis set), with the cut-off energy for real-space mesh of 400 Ry. Brillouin-zone integration is performed by Monkhorst-Pack scheme[28] with $12 \times 12 \times 6$ k-point grid. The unit-cell parameters and internal coordinates are optimized by the total-energy minimization and used for the electronic structure calculations. When our cal-

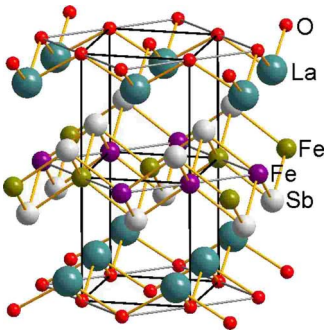

FIG. 1. (Color online) Atomic structure of LaFeSbO. In this structure, LaO and FeSb layers alternate along the c direction. Black lines represent the tetragonal unit cell of the NM phase and $\sqrt{2}\times\sqrt{2}$ supercell is also indicated in gray lines. The Fe spin configuration in the SDW phase is shown with different colors of Fe atoms.

culational method is applied to LaZnPnO (Pn=P, As, and Sb), as a test, the obtained structural parameters are in good agreement with experimentally known values.

Oxypnictide compounds have layered structure with alternating LaO and FePn layers along the c axis, as shown in Fig. 1. In the FePn layer Fe atoms form a two-dimensional square lattice and are fourfold coordinated with Pn atoms to form a network of tetrahedrons, and the LaO layer is in structural analogy with FePn layer with Fe and Pn atoms replaced by O and La atoms, respectively. LaFeAsO is known to have two structural phases of different symmetries with a transition temperature of ~150 K (Refs. 9 and 10) as mentioned earlier. The higher-temperature phase has tetragonal $P4/nmm$ symmetry and the lower-temperature one has monoclinic $P112/n$ or equivalently orthorhombic $Cmma$.[29]

To optimize the structure of LaFeSbO as well as LaFePO and LaFeAsO, we choose a $\sqrt{2}\times\sqrt{2}\times 2$ supercell of the original tetragonal $(1\times 1\times 1)$ primitive unit cell for the starting structure and fully relax the structure including the cell parameters. We choose the doubled unit cell along the c axis to examine the experimentally observed spin configuration in LaFeAsO that the spin direction is opposite between two adjacent Fe layers along the c axis.[9] With this choice of the supercell, we perform both the NM calculation and spin-polarized one with the well-known SDW spin configuration as represented in Fig. 1.

The optimized cell parameters and atomic coordinates of LaFeSbO are listed in Table I along with those for LaFePO and LaFeAsO for comparison. For all of the compounds, our NM calculations result in tetragonal structures with $a=b$ and the lattice parameters of LaFeSbO are slightly larger than those of LaFeAsO as expected. The NM-phase tetragonal structure is not stable with respect to AFM spin orderings. Our spin-polarized calculation for the SDW phase leads to an orthorhombic unit cell with $a\neq b$ and again LaFeSbO is found to have larger lattice parameters than LaFeAsO. Our result for LaFeAsO is consistent with the previous calculation[29] which shows that in the SDW spin configuration, parallel spins tend to get closer and opposite spins move apart by structural distortion with slightly increased γ angle (between a and b axes in the original 1×1 unit cell) from 90° to lift the magnetic frustration. The γ angles from our structure optimization are found to be 90.7°, 90.9°, and 91.1°, for Pn=P, As, and Sb, respectively. The angle of 90.9° for LaFeAsO is in reasonable agreement with the measured value of 90.3°,[9] supporting the validity of our predicted value for LaFeSbO. Moreover, the increasing γ angle from P to Sb is also consistent with the fact that the calculated Fe spin moment increases monotonically from P to Sb, as presented below.

The AFM spin configuration (Fig. 1) in the optimized orthorhombic unit cell is more stable than the NM phase in the optimized tetragonal unit cell by 153, 354, and 706 meV per formula unit for phosphide, arsenide, and antimonide, respectively. The local magnetic moment on a Fe atom is also increasing as 2.42, 2.83, and 3.13μ_B. Therefore, the magnetism is greatly enhanced in the LaFeSbO compared

TABLE I. Calculated structural parameters, DOS at E_f [$N(E_f)$], and Fe magnetic moment (m) of LaFePnO for Pn=P, As, and Sb. In the SDW phase, the Fe atoms of the same spin are located along the b_o axis. Iron (oxygen) atoms are located at $z=0.5$ ($z=0$) along the c axis.

NM (tetragonal, $P4/nmm$)						
Pn	a (Å)	b (Å)	c (Å)	z(La)	z(Pn)	$N(E_f)$
P	3.972	3.972	8.590	0.153	0.624	4.5
As	3.999	3.999	8.706	0.145	0.640	1.7
Sb	4.106	4.106	9.311	0.130	0.659	2.9
SDW (orthorhombic, $Cmma$)						
Pn	a_o (Å)	b_o (Å)	c (Å)	z(La)	z(Pn)	$m(\mu_B)$
P	5.741	5.672	8.641	0.150	0.634	2.42
As	5.780	5.693	8.875	0.139	0.654	2.83
Sb	5.955	5.844	9.542	0.124	0.673	3.13

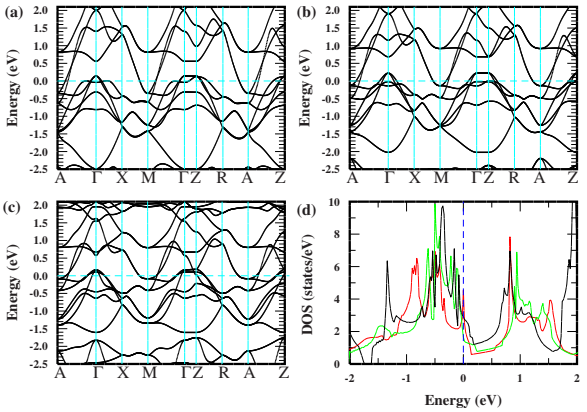

FIG. 2. (Color online) Calculated band structures of (a) LaFePO, (b) LaFeAsO, and (c) LaFeSbO for NM phase. In (d), DOSs are shown in red (dark gray), green (gray), and black colors for LaFePO, LaFeAsO, and LaFeSbO, respectively.

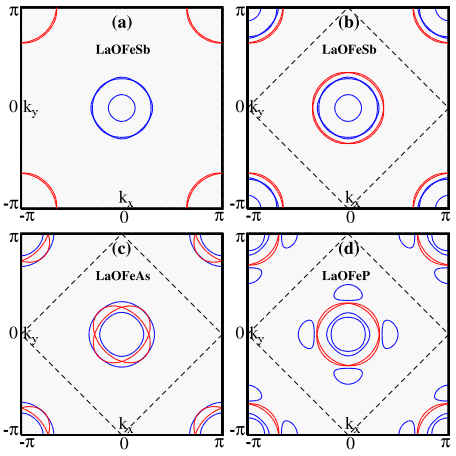

FIG. 3. (Color online) Calculated Fermi surfaces in the NM phase. (a) LaFeSbO using the primitive unit cell and (b) LaFeSbO, (c) LaFeAsO, and (d) LaFePO using the $\sqrt{2}\times\sqrt{2}$ supercell. Hole pockets are represented in blue (dark gray) and electron pockets are in red (gray). In (b)–(d), the dashed lines represent the Brillouin zone of the $\sqrt{2}\times\sqrt{2}$ supercell.

with LaFeAsO and LaFePO.[30] In the meanwhile, no ferromagnetic (FM) solution is found in our calculation.

Figure 2 shows the band structures calculated in the NM phase for the series of oxypnictides. Complicated Fe d-derived bands exist near E_f with electron and hole pockets around M and Γ points, respectively, and dispersionless bands between Γ and Z points, indicating the two-dimensionality of the layered structure. Although overall features are similar qualitatively among Pn species, bandwidths and detailed energy positions of Fe d-derived bands are different among pnictides.

As shown in Fig. 2, the band dispersion is considerably different among the compounds. The P compound has largest dispersion and bandwidth and then follow the As and Sb compounds, as is easily seen, for example, for the electron bands at M point near E_f. The decreasing dispersion from P to Sb compounds is easily understood by the increasing Pn atomic size and distance between Fe and neighboring Pn atoms, which results in reduced orbital overlap between them and therefore the localization of Fe d states. The localization of Fe d states close to the atomic-orbital limit enhances the intra-atomic exchange coupling or the Hund's rule coupling, so that the Fe local spin moment and the stability of magnetic solution are expected to increase from P to Sb. Our results presented above are consistent with this expectation.

Detailed energy positions of Fe d-derived bands are different among pnictides (Fig. 2) and this affects the number of hole pockets around the Γ point. Energy splittings between two d_{z^2}-derived bands (which have finite dispersion along the Γ-Z line) and between d_{xy} and $d_{yz}+d_{zx}$ derived bands (which are dispersionless along the Γ-Z line) decrease from P to Sb. As a result, there are three bands crossing the E_f near the Γ point in the case of LaFeSbO while there are only two bands in the cases of LaFePO and LaFeAsO. The three-dimensional (3D) hole pocket centered around the Z point, which is present in LaFePO and LaFeAsO, is absent in LaFeSbO. This will be discussed in detail later with Fig. 3.

Figure 2(d) shows the density of states (DOS) of LaFePO, LaFeAsO, and LaFeSbO in the NM phase. The value of DOS at E_f is 2.9 states/eV per formula unit in LaFeSbO, which is much greater than 1.7 states/eV in LaFeAsO. This implies that SDW formation and superconductivity may occur more effectively in LaFeSbO than LaFeAsO, since large DOS at E_f often results in stronger instability of the Fermi surface. In the case of LaFePO, DOS at E_f is as large as 4.5 states/eV due to a very narrow peak right at E_F originating from Van Hove singularities which are away from the Γ or M point, so substantial part of DOS may not contribute strongly to the superconductivity within the spin-fluctuation scenario. In the case of the SDW phase, the electronic structure near E_f is drastically changed from the NM phase. The DOS at E_f is greatly reduced to 0.23 states/eV for the SDW phase due to the SDW gap formation. The SDW phase is still metallic, however, with a finite DOS value at E_f, as the nesting is not perfect as in the case of LaFeAsO system.[11]

The Fermi surface of LaFeSbO is shown in Fig. 3 on the $k_z=0$ plane. The Fermi surfaces of LaFeAsO and LaFePO are also shown for comparison. Similarly to the LaFeAsO and LaFePO cases, there are hole pockets around the Γ point and electron pockets near the M point in LaFeSbO. In this case, however, there is additional small hole Fermi surface centered at Γ which is absent in LaFeAsO and LaFePO, as a result of different Fe d band distributions near E_f (see Fig. 2). Therefore, LaFeSbO has three hole pockets near the Γ point and two electron pockets around the M point. All Fermi surfaces are cylindrical. The small hole surface at Γ has a different orbital character from the 3D hole pocket at Z in LaFeAsO and LaFePO. The nesting between electron and hole Fermi surfaces defined by the (π,π) vector in the reciprocal space is also manifest in this case. In order to make comparison straightforward, Figs. 3(b)–3(d) show the original Fermi surfaces and those shifted by the $(\pm\pi,\pm\pi)$ vectors. As shown in Fig. 3(b), the shapes of Fermi surfaces in LaFeSbO are quite close to circles compared with those in LaFeAsO and LaFePO and the radii of circular surfaces match closely between the hole and electron surfaces. Furthermore, the electron surfaces coincide with each other al-

most perfectly and so do the two hole surfaces at Γ. We also estimated Pauli susceptibility $[\chi_0(\pi,\pi)]$ with constant matrix elements and the result is greatest for LaFeSbO. These features clearly indicate an enhanced nesting between the Fermi surfaces of LaFeSbO compared with LaFeAsO and LaFePO.

Within the framework of spin-fluctuation-mediated superconductivity which is widely accepted for iron arsenides,[31,32] strong superconductivity occurs if electrons couple strongly with the spin fluctuation of $q=(\pi,\pi)$. In general, superconductivity becomes stronger if DOS at E_f is greater. Our calculations show that in LaFeSbO, DOS at E_f is almost doubled, nesting feature of the Fermi surface is enhanced, and the SDW phase becomes energetically more stable and has an increased magnetization of iron compared with LaFeAsO. These results indicate stronger electron-spin-fluctuation coupling in LaFeSbO, which is necessary for higher T_c. Thus, within the current understanding of these materials, LaFeSbO is a very attractive candidate for a superconductor with a higher T_c.

In summary, we have investigated the basic physical properties of a hypothetical iron-based oxypnictide compound LaFeSbO by first-principles calculations. It is predicted that the compound favors to be in the tetragonal crystal structure with $a=b$ in the NM state while orthorhombic structure with $a\neq b$ is the lowest-energy structure in the stripe-type AFM-SDW phase. The SDW phase becomes more stable, having the local spin moments on Fe atoms and the total-energy difference between the SDW and NM phase larger than those in LaFeAsO. In the NM phase, the band dispersion around E_f is substantially reduced, increasing DOS at E_f greatly. The calculated Fermi surface in the NM-phase LaFeSbO exhibits enhanced nesting feature between the hole and electron surfaces with the nesting vector (π,π) for the SDW formation.

This work was supported by the KRF (Grant No. KRF-2007-314-C00075) and by the KOSEF under Grant No. R01-2007-000-20922-0. Computational resources were provided by KISTI Supercomputing Center (Grant No. KSC-2008-S02-0004).

*h.j.choi@yonsei.ac.kr

[1] Y. Kamihara, H. Hiramatsu, M. Hirano, R. Kawamura, H. Yanagi, T. Kamiya, and H. Hosono, J. Am. Chem. Soc. **128**, 10012 (2006).
[2] Y. Kamihara, T. Watanabe, M. Hirano, and H. Hosono, J. Am. Chem. Soc. **130**, 3296 (2008).
[3] H. Takahashi, K. Igawa, K. Arii, Y. Kamihara, M. Hirano, and H. Hosono, Nature (London) **453**, 376 (2008).
[4] G. Giovannetti, S. Kumar, and J. van den Brink, Physica B **403**, 3653 (2008).
[5] D. J. Singh and M.-H. Du, Phys. Rev. Lett. **100**, 237003 (2008).
[6] K. Haule, J. H. Shim, and G. Kotliar, Phys. Rev. Lett. **100**, 226402 (2008).
[7] G. Xu, W. Ming, Y. Yao, X. Dai, S. Zhang, and Z. Fang, Europhys. Lett. **82**, 67002 (2008).
[8] I. I. Mazin, M. D. Johannes, L. Boeri, K. Koepernik, and D. J. Singh, arXiv:0806.1869 (unpublished).
[9] C. de la Cruz, Q. Huang, J. W. Lynn, J. Li, W. Ratcliff II, J. L. Zarestky, H. A. Mook, G. F. Chen, J. L. Luo, N. L. Wang, and P. Dai, Nature (London) **453**, 899 (2008).
[10] H. H. Klauss, H. Luetkens, R. Klingeler, C. Hess, F. J. Litterst, M. Kraken, M. M. Korshunov, I. Eremin, S. L. Drechsler, R. Khasanov, A. Amato, J. Hamann-Borrero, N. Leps, A. Kondrat, G. Behr, J. Werner, and B. Büchner, Phys. Rev. Lett. **101**, 077005 (2008).
[11] J. Dong, H. J. Zhang, G. Xu, Z. Li, G. Li, W. Z. Hu, D. Wu, G. F. Chen, X. Dai, J. L. Luo, Z. Fang, and N. L. Wang, Europhys. Lett. **83**, 27006 (2008).
[12] Y. Nakai, K. Ishida, Y. Kamihara, M. Hirano, and H. Hosono, arXiv:0804.4765, J. Phys. Soc. Jpn. (to be published).
[13] B. Lorenz, K. Sasmal, R. P. Chaudhury, X. H. Chen, R. H. Liu, T. Wu, and C. W. Chu, Phys. Rev. B **78**, 012505 (2008).
[14] V. Cvetkovic and Z. Tesanovic, arXiv:0804.4678 (unpublished).
[15] M. M. Korshunov and I. Eremin, Phys. Rev. B **78**, 140509(R) (2008).
[16] Z. P. Yin, S. Lebegue, M. J. Han, B. P. Neal, S. Y. Savrasov, and W. E. Pickett, Phys. Rev. Lett. **101**, 047001 (2008).
[17] Z.-A. Ren, W. Lu, J. Yang, W. Yi, X.-L. Shen, Z.-C. Li, G.-C. Che, X.-L. Dong, L.-L. Sun, F. Zhou, and Z.-X. Zhao, Chin. Phys. Lett. **25**, 2215 (2008).
[18] G. F. Chen, Z. Li, D. Wu, G. Li, W. Z. Hu, J. Dong, P. Zheng, J. L. Luo, and N. L. Wang, Phys. Rev. Lett. **100**, 247002 (2008).
[19] Z.-A. Ren, J. Yang, W. Lu, W. Yi, G.-C. Che, X.-L. Dong, L.-L. Sun, and Z.-X. Zhao, Mater. Res. Innovations **12**, 105 (2008).
[20] Z.-A. Ren, J. Yang, W. Lu, W. Yi, X.-L. Shen, Z.-C. Li, G.-C. Che, X.-L. Dong, L.-L. Sun, F. Zhou, and Z.-X. Zhao, Europhys. Lett. **82**, 57002 (2008).
[21] J. Yang, Z.-C. Li, W. Lu, W. Yi, X.-L. Shen, Z.-A. Ren, G.-C. Che, X.-L. Dong, L.-L. Sun, F. Zhou, and Z.-X. Zhao, Supercond. Sci. Technol. **21**, 082001 (2008).
[22] M. Rotter, M. Tegel, D. Johrendt, I. Schellenberg, W. Hermes, and R. Pöttgen Phys. Rev. B **78**, 020503(R) (2008).
[23] M. Rotter, M. Tegel, and D. Johrendt, Phys. Rev. Lett. **101**, 107006 (2008).
[24] C. Krellner, N. Caroca-Canales, A. Jesche, H. Rosner, A. Ormeci, and C. Geibel, Phys. Rev. B **78**, 100504(R), (2008).
[25] G. F. Chen, Z. Li, G. Li, W. Z. Hu, J. Dong, X. D. Zhang, P. Zheng, N. L. Wang, and J. L. Luo, Chin. Phys. Lett. **25**, 3403 (2008).
[26] J. P. Perdew, K. Burke, and M. Ernzerhof, Phys. Rev. Lett. **77**, 3865 (1996).
[27] D. Sanchez-Portal, P. Ordejon, E. Artacho, and J. M. Soler, Int. J. Quantum Chem. **65**, 453 (1997).
[28] H. J. Monkhorst and J. D. Pack, Phys. Rev. B **13**, 5188 (1976).
[29] T. Yildirim, Phys. Rev. Lett. **101**, 057010 (2008).
[30] Although calculated local-density approximation (LDA) or GGA magnetic moments in FeAs compounds are greater than measured values and sensitive to the As position (see, e.g., Refs. 8 and 16), the substantial difference in our magnetic moments for different pnictides supports the general trend.
[31] I. I. Mazin, D. J. Singh, M. D. Johannes, and M. H. Du, Phys. Rev. Lett. **101**, 057003 (2008).
[32] K. Kuroki, S. Onari, R. Arita, H. Usui, Y. Tanaka, H. Kontani, and H. Aoki, Phys. Rev. Lett. **101**, 087004 (2008).